Journal of Carcinogenesis
Covering Genesis to Therapeutics

Journal of Carcinogenesis, ISSN: 1477-3163
2025; Vol 24: Issue 2s, https://carcinogenesis.com/

Formulation, Characterization, and In Vitro Cytotoxic Evaluation of Etoposide-Loaded Nanobubbles for Enhanced Cancer Chemotherapy

Nikunj Solanki[1], Chand Kaur[2], Sonal Solanki[3*], Shivanee Vyas[4], B. R. Asokan[5], Prem Shankar Gupta[6], Brijesh Sharma[7], Neelam Pawar[8]

[1,3]Department of Pharmaceutics, HSBPVT's, Group of Institutions, Faculty of Pharmacy, Kashti, Ta- Shrigonda, Ahilyanagar, Maharastra. Pin - 414701.

[2]Geeta Institute of Pharmacy, Geeta University, 132145.

[4]Department of Pharmaceutics, Oriental College of Pharmacy, Bhopal 462021.

[5]Department of Pharmacology, TSRMMCH & RC (The Tamilnadu Dr. MGR, Medical Univ., Chennai), Irungalur, Trichy-621 105, India.

[6]Department of Pharmaceutics, Teerthanker Mahaveer College of Pharmacy, Teerthanker Mahaveer University, Moradabad.

[7]Institute of Biomedical Education and Research Department of Pharmacy Mangalayatan University Aligarh India Pin-202145.

[8]Department of Pharmaceutical Sciences, Chaudhary Bansi Lal University, Prem Nagar, Bhiwani Haryana-127031.

***Corresponding Author:**

Sonal Solanki

HSBPVT's, Group of Institutions, Faculty of Pharmacy, Kashti, Ta- Shrigonda, Ahilyanagar, Maharastra. Pin - 414701.

Email ID - drsonalsolanki25@gmail.com

ABSTRACT

This study aimed to develop, characterize, and evaluate the in vitro cytotoxic potential of Etoposide-loaded nanobubbles for enhanced cancer therapy. Nanobubbles were formulated using a thin-film hydration technique followed by probe sonication, employing phosphatidylcholine, cholesterol, and PEG-4000 as the lipid matrix. Five formulations (F1–F5) were developed with varying lipid concentrations and characterized for particle size, zeta potential, polydispersity index (PDI), entrapment efficiency, and drug loading. The optimized formulation (F5) exhibited a particle size of 125.5 ± 2.1 nm, zeta potential of –30.6 ± 0.7 mV, and entrapment efficiency of 91.4 ± 1.1%. In vitro release studies revealed a sustained drug release pattern over 48 hours, with F5 achieving 99.4 ± 0.6% release. Kinetic modelling confirmed a first-order release mechanism with non-Fickian diffusion behaviour. Cytotoxicity studies using the MTT assay were performed on MCF-7 (breast), A549 (lung), and HeLa (cervical) cancer cell lines. The Etoposide-loaded nanobubbles demonstrated significantly enhanced cytotoxicity compared to free drug, with lower IC_{50} values in all tested cell lines, while blank nanobubbles showed negligible toxicity. These findings support the potential of nanobubble-based systems for targeted and controlled delivery of chemotherapeutic agents, offering improved therapeutic efficacy and reduced systemic toxicity.

Keywords: *Etoposide, Nanobubbles, Controlled drug release, Cytotoxicity, Cancer drug delivery*

How to Cite: Nikunj Solanki, Chand Kaur, Sonal Solanki, Shivanee Vyas, B. R. Asokan, Prem Shankar Gupta, Brijesh Sharma, Neelam Pawar, (2025) Expression Time and Peak Concentration Dendritic Cells, Perforin, and Granzyme B in Invivo and Invitro Studies: A Systematic Review, *Journal of Carcinogenesis*, *Vol.24, No.2s*, 666-677

1. INTRODUCTION

Cancer remains one of the leading causes of mortality worldwide, accounting for millions of deaths annually despite significant advancements in diagnosis and treatment. Chemotherapy continues to play a central role in cancer management; however, its effectiveness is often limited by systemic toxicity, poor drug solubility, multidrug resistance, and lack of target specificity. These drawbacks not only compromise patient outcomes but also affect the quality of life during therapy. Hence, there is a pressing need to develop more efficient and safer drug delivery systems that can enhance the therapeutic index of chemotherapeutic agents (Cordani et al., 2024; Dolgin, 2021; Hausman, 2019; Kroemer & Pouyssegur, 2008).

Etoposide, a semisynthetic derivative of podophyllotoxin, is widely used in the treatment of various malignancies including lung cancer, testicular cancer, lymphomas, and certain leukemias. It acts primarily by inhibiting the enzyme topoisomerase II, thereby inducing DNA strand breaks and apoptosis in rapidly dividing cancer cells (Bailly, 2023; Hainsworth & Greco, 1995; Hande, 1992; Issell & Crooke, 1979). Despite its potent antitumor activity, the clinical use of Etoposide is hampered by poor aqueous solubility, low oral bioavailability, dose-limiting toxicities, and nonspecific biodistribution. These limitations necessitate the development of novel

delivery strategies to maximize its therapeutic efficacy while minimizing systemic side effects (Kroemer & Pouyssegur, 2008; Roy & Saikia, 2016).

Nanotechnology-based drug delivery systems have emerged as a transformative approach to overcome the limitations of conventional chemotherapy. Among the various nanocarriers explored, nanobubbles have recently gained attention due to their unique structural and functional attributes. Nanobubbles are gas-filled, nanosized vesicles typically composed of a lipid or polymeric shell surrounding a core of gas, such as perfluoropropane. Their small size, enhanced surface area, and ability to encapsulate both hydrophilic and hydrophobic drugs make them attractive candidates for controlled and targeted drug delivery. Additionally, nanobubbles can be designed to be responsive to external stimuli such as ultrasound, which can facilitate site-specific drug release and improve therapeutic outcomes (Ahsan et al., 2024; Charbgoo et al., 2017; Cui & Smith, 2022; Rajakumar & Abdul Rahuman, 2011). One of the key advantages of nanobubbles over traditional nanoparticles is their echogenic property, which allows for concurrent drug delivery and ultrasound imaging. This dual functionality holds promise for image-guided therapy and real-time monitoring of treatment response. Furthermore, the gaseous core of nanobubbles can serve as a contrast agent in ultrasound imaging, making them highly suitable for theranostic applications. By tailoring the surface composition and size, nanobubbles can achieve prolonged circulation time, reduced clearance by the reticuloendothelial system (RES), and enhanced accumulation in tumor tissues via the enhanced permeability and retention (EPR) effect (Hashida, 2022; Markman et al., 2013; Shi et al., 2020).

In the context of Etoposide delivery, encapsulation within nanobubbles presents a compelling strategy to address its pharmacokinetic and pharmacodynamic limitations. Encapsulated Etoposide is protected from premature degradation and clearance, ensuring higher stability and sustained release at the target site. Moreover, the lipid shell can be engineered to improve cellular uptake and endosomal escape, further enhancing drug bioavailability within cancer cells. Preliminary studies have shown that nanobubble-mediated drug delivery can significantly improve the therapeutic index of chemotherapeutics and reduce systemic toxicity in preclinical cancer models (Bailly, 2023; Fleming et al., 1989). Despite the promising features, the formulation and characterization of nanobubbles require careful optimization to achieve desirable physicochemical and biological properties. Parameters such as particle size, surface charge (zeta potential), polydispersity index (PDI), encapsulation efficiency, and drug release kinetics must be meticulously controlled to ensure consistency, stability, and reproducibility. Additionally, cytotoxicity assessments on various cancer cell lines are essential to evaluate the therapeutic potential and safety profile of the developed system. This study focuses on the formulation, characterization, and in vitro cytotoxic evaluation of Etoposide-loaded nanobubbles. A systematic approach was adopted to prepare nanobubbles using the thin-film hydration technique followed by sonication, incorporating phosphatidylcholine, cholesterol, and PEG-4000 as primary excipients. The formulations were analyzed for particle size, zeta potential, PDI, entrapment efficiency, drug loading, and in vitro drug release behavior. Furthermore, the cytotoxic effect of the optimized nanobubbles was investigated using MTT assay on three cancer cell lines: MCF-7 (breast cancer), A549 (lung cancer), and HeLa (cervical cancer) (Bailly, 2023; Fleming et al., 1989){Kroemer, 2008 #312;Roy, 2016 #310;Cordani, 2024 #315}.

The rationale behind selecting these three cell lines lies in their relevance to Etoposide's clinical use and their distinct biological characteristics. MCF-7 represents hormone-responsive breast cancer, A549 is a model for non-small cell lung cancer, and HeLa is a well-characterized cervical cancer line. Studying the nanobubble efficacy across these models enables a broader understanding of their therapeutic applicability. The novelty of this work lies in integrating nanobubble technology with Etoposide delivery to achieve enhanced anticancer activity with reduced toxicity. By systematically evaluating the physicochemical attributes and biological effects of the nanobubble formulations, this research aims to establish a foundation for future translational development of nanobubble-based chemotherapeutic systems. Ultimately, the successful implementation of this strategy could pave the way for more effective, targeted, and personalized cancer therapies.

In summary, this study addresses a critical gap in cancer therapeutics by designing a nanocarrier system tailored to improve the pharmacological profile of Etoposide. Through comprehensive in vitro evaluations and comparative analysis across multiple cell lines, the study seeks to demonstrate the superiority of nanobubble-mediated drug delivery over conventional free drug administration. The findings are expected to contribute valuable insights toward the advancement of Nano formulation platforms for cancer treatment, particularly in the realm of precision medicine and minimally invasive therapy.

2. MATERIALS AND METHODS

2.1. Materials

Etoposide, a chemotherapeutic agent known for its potent anti-proliferative activity, was procured as a high-purity standard from a licensed pharmaceutical supplier for research purposes. The lipids used in the nanobubble formulation, specifically

L-α-phosphatidylcholine and cholesterol, were of analytical grade and purchased from Sigma-Aldrich (USA), ensuring high-quality membrane-forming components for stable vesicle formation. Polyethylene glycol 4000 (PEG-4000), a hydrophilic polymer used to enhance the steric stabilization and circulation time of nanobubbles, was also acquired from Sigma-Aldrich. Ethanol, employed as a solvent for lipid dissolution, and phosphate-buffered saline (PBS, pH 7.4), used for hydration of the lipid film, were obtained from HiMedia Laboratories, India. The PBS served as a physiologically relevant medium to simulate in vivo conditions during formulation and in vitro studies. Perfluoropropane gas, an inert and low-solubility gas, was employed to saturate the core of the nanobubbles, facilitating acoustic responsiveness and enhanced stability. All other reagents and solvents used in the study were of analytical grade, stored under recommended conditions, and used without further purification to maintain the integrity and reproducibility of the formulation process.

2.2. Preparation of Etoposide-Loaded Nanobubbles

Etoposide-loaded nanobubbles were prepared using a modified thin-film hydration technique followed by probe sonication, ensuring uniform entrapment and nanoscale dispersion. Based on the composition detailed in Table 1, accurately weighed amounts of Etoposide (5 mg), phosphatidylcholine (100–180 mg), cholesterol (50–90 mg), and PEG-4000 (20 mg) were dissolved in 10 mL of ethanol to prepare a clear and homogenous organic solution. This mixture was transferred into a clean, dry 250 mL round-bottom flask and subjected to rotary evaporation under reduced pressure at 40 ± 2°C using a Buchi-type rotary evaporator. A consistent and uniform thin lipid film was formed on the inner surface of the flask over 25–30 minutes, ensuring complete removal of ethanol. The dried lipid film was then hydrated with 10 mL of phosphate-buffered saline (PBS, pH 7.4), which had been previously saturated with perfluoropropane gas to enable the formation of gas-filled nanobubbles. The hydration was performed with gentle agitation for 30 minutes to allow complete detachment and dispersion of the lipid film into the aqueous phase. The resulting coarse dispersion was then subjected to high-energy probe sonication at a frequency of 20 kHz for 5 minutes, using pulse mode (30 seconds on, 10 seconds off) in an ice bath to avoid thermal degradation of the drug or lipids. This sonication step led to the breakdown of multilamellar vesicles into uniformly distributed, gas-core nanobubbles encapsulating Etoposide within their lipid shell. The prepared nanobubble dispersion was stored in amber glass vials at 4°C and further used for characterization, in vitro release, and cytotoxicity studies {Cavalli, 2015 #328; Peng, 2019 #327; Odziomek, 2022 #329}.

Table 1. Composition of Etoposide-Loaded Nanobubble Formulations

Formulation Code	Etoposide (mg)	Phosphatidylcholine (mg)	Cholesterol (mg)	PEG-4000 (mg)	Hydration Medium (PBS, mL)	Perfluoropropane Gas
F1	5	100	50	20	10	Saturated
F2	5	120	60	20	10	Saturated
F3	5	140	70	20	10	Saturated
F4	5	160	80	20	10	Saturated
F5	5	180	90	20	10	Saturated

2.3. Characterization of Nanobubbles

2.3.1. Particle Size, Polydispersity Index (PDI), and Zeta Potential

The average particle size, polydispersity index (PDI), and zeta potential of the Etoposide-loaded nanobubbles were evaluated using Dynamic Light Scattering (DLS), a well-established technique for analyzing nanoparticulate dispersion characteristics. The measurements were performed using a Zetasizer Nano ZS90 (Malvern Instruments, UK), which utilizes laser backscatter detection at a fixed angle of 90° to determine the hydrodynamic diameter and size distribution profile of colloidal systems. Prior to measurement, a small aliquot of the nanobubble dispersion was carefully diluted 1:10 with double-distilled water to reduce the opacity and minimize multiple scattering phenomena, ensuring accurate and reproducible readings. The diluted sample was transferred into a disposable cuvette and equilibrated at 25 ± 0.5°C before analysis. The PDI values provided insight into the uniformity of the nanobubble population, with values below 0.3 indicating a monodisperse and stable formulation. Zeta potential measurements were performed in folded capillary cells using the same instrument to assess the surface charge of the nanobubbles. The surface charge is a critical indicator of colloidal stability, as it influences interparticle repulsion and aggregation behavior. A zeta potential magnitude greater than ±25 mV was considered indicative of good electrostatic stabilization. All measurements were conducted in triplicate, and the results were expressed as mean ± standard deviation (SD) {Cavalli, 2015 #328; Peng, 2019 #327; Odziomek, 2022 #329}.

2.3.2. Surface Morphology (TEM Analysis)

The morphological characteristics of the Etoposide-loaded nanobubbles were assessed using Transmission Electron

Microscopy (TEM), a powerful imaging tool that provides high-resolution visualization of nanoscale structures. This analysis was performed to confirm the size, shape, and structural integrity of the prepared nanobubbles. For sample preparation, a drop of freshly prepared nanobubble suspension was carefully placed onto a carbon-coated copper grid using a micropipette. The sample was allowed to settle for 1–2 minutes to enable proper adhesion of the vesicles to the grid surface. Excess liquid was gently blotted using filter paper, after which the sample was negatively stained with 1% (w/v) phosphotungstic acid (PTA) to enhance contrast and improve visibility of the nanobubble outlines under the electron beam. The grid was then allowed to air-dry at room temperature in a dust-free environment. Once dried, the grids were examined under a TEM operated at an accelerating voltage of 80–120 kV. Images were captured at various magnifications to assess the shape (spherical or ellipsoidal), boundary integrity, and dispersion of the nanobubbles. The formulation was expected to exhibit smooth-surfaced, spherical structures with uniform distribution, indicative of successful nanobubble formation. All TEM observations were performed in triplicate, and representative images were used to correlate visual data with particle size measurements obtained from DLS {Cavalli, 2015 #328; Peng, 2019 #327; Odziomek, 2022 #329}.

2.3.3. Entrapment Efficiency and Drug Loading

The entrapment efficiency (EE%) and drug loading (DL%) of Etoposide-loaded nanobubbles were quantitatively determined to evaluate the formulation's encapsulation performance. These parameters are crucial for assessing how effectively the drug is incorporated into the lipid shell of the nanobubbles. To separate the unencapsulated (free) Etoposide from the drug-loaded nanobubbles, 5 mL of the freshly prepared dispersion was subjected to ultracentrifugation at 15,000 rpm for 30 minutes at 4°C using a high-speed refrigerated centrifuge. This process allowed the nanobubbles to sediment while the free, unentrapped drug remained in the supernatant. The collected supernatant was carefully withdrawn and analyzed spectrophotometrically using a UV-Visible spectrophotometer (Shimadzu, Japan) at a wavelength of 285 nm, which corresponds to the maximum absorbance (λmax) of Etoposide. A standard calibration curve of Etoposide in PBS (pH 7.4) was used to determine the drug concentration in the supernatant. The amount of drug successfully encapsulated was calculated by subtracting the amount of free drug (in the supernatant) from the total drug initially added during formulation. Entrapment efficiency and drug loading were calculated using the formulas {Cavalli, 2015 #328; Peng, 2019 #327; Odziomek, 2022 #329}:

- **Entrapment Efficiency (%)** = (Entrapped Drug / Total Drug Added) × 100
- **Drug Loading (%)** = (Entrapped Drug / Total Weight of Nanobubbles) × 100

All measurements were performed in triplicate, and the results were reported as mean ± standard deviation (SD).

2.4. In Vitro Drug Release Study

The in vitro release profile of Etoposide from the nanobubble formulations was investigated using the dialysis bag diffusion technique, a standard method suitable for evaluating the release behavior of nanoparticulate drug delivery systems. This method simulated physiological conditions to predict the release kinetics of the encapsulated drug over time. A fixed volume (2 mL) of the Etoposide-loaded nanobubble dispersion was carefully transferred into a pre-activated dialysis membrane (molecular weight cut-off: 12–14 kDa), which was securely sealed at both ends. The dialysis bag was then placed in a glass beaker containing 100 mL of phosphate-buffered saline (PBS, pH 7.4), serving as the release medium. The entire system was maintained at a physiological temperature of 37 ± 0.5°C using a thermostatically controlled water bath with a constant stirring speed of 100 rpm to ensure sink conditions and uniform drug diffusion. At predetermined time intervals (0.5, 1, 2, 4, 6, 8, 12, 24, and 48 hours), 2 mL aliquots of the external medium were withdrawn for analysis and immediately replaced with an equal volume of fresh PBS to maintain the volume and concentration gradient. The collected samples were analyzed for Etoposide content using a UV-Visible spectrophotometer at 285 nm, the λmax of Etoposide, against a reagent blank. A calibration curve was prepared using standard Etoposide solutions in PBS to quantify the amount of drug released at each time point. All release experiments were conducted in triplicate, and the cumulative percentage of drug release was calculated and plotted against time to evaluate the release kinetics. Further, the release data were fitted to various mathematical models (zero-order, first-order, Higuchi, and Korsmeyer-Peppas) to determine the mechanism of drug release {Cavalli, 2015 #328; Odziomek, 2022 #329; Ghasemzadeh, 2023 #326}.

2.5. In Vitro Cytotoxicity Assessment (MTT Assay) in MCF-7

The cytotoxic potential of the Etoposide-loaded nanobubble formulations was assessed using the well-established MTT assay, which evaluates cell viability based on mitochondrial metabolic activity. The assay was conducted on MCF-7 human breast adenocarcinoma cells, a commonly used cell line for anticancer drug screening due to its sensitivity to chemotherapeutic agents. MCF-7 cells were cultured in Dulbecco's Modified Eagle Medium (DMEM) supplemented with 10% fetal bovine serum (FBS) and 1% penicillin–streptomycin solution. Cells were maintained at 37°C in a humidified atmosphere containing 5% CO_2. For the assay, cells were harvested during the logarithmic growth phase and seeded into 96-well flat-bottom plates at a density of 1×10^4 cells per well in 100 µL of complete medium. The plates were incubated for 24 hours to allow proper cell attachment. Following attachment, the culture medium was carefully aspirated and replaced with 100 µL of fresh medium containing varying concentrations (10, 25, 50, 75, and 100 µg/mL) of Etoposide-loaded nanobubbles, free Etoposide, or blank nanobubbles as controls. Untreated wells served as the negative control

(100% viability). The cells were incubated with test samples for 48 hours under standard culture conditions. After the treatment period, 20 µL of MTT solution (5 mg/mL in PBS) was added to each well and incubated for an additional 4 hours to allow the formation of insoluble formazan crystals by viable, metabolically active cells. Post incubation, the medium was carefully removed, and 100 µL of dimethyl sulfoxide (DMSO) was added to each well to solubilize the purple formazan crystals. The absorbance of the resulting solution was measured at 570 nm using a microplate reader (Bio-Rad iMark or equivalent) {Präbst, 2017 #330;Pascua-Maestro, 2018 #331}.
Cell viability (%) was calculated using the formula:
Cell Viability (%) = {Absorbance of Treated Cells / Absorbance of Control Cells} ×100
The cytotoxicity profile of each formulation was plotted as a dose-response curve, and the half-maximal inhibitory concentration (IC_{50}) values were determined using non-linear regression analysis. All experiments were conducted in triplicate, and the results were presented as mean ± standard deviation (SD).

2.5.1. In Vitro Cytotoxicity Assay on A549 and HeLa Cell Lines

In addition to MCF-7, the cytotoxic potential of Etoposide-loaded nanobubbles was evaluated against two additional human cancer cell lines: A549 (lung carcinoma) and HeLa (cervical cancer) using the MTT assay. Both cell lines were obtained from a certified cell repository and maintained under standard culture conditions. A549 cells were cultured in Ham's F-12K medium, while HeLa cells were maintained in Minimum Essential Medium (MEM), each supplemented with 10% fetal bovine serum (FBS) and 1% penicillin–streptomycin. Cells were incubated at 37 ± 1°C in a 5% CO_2 humidified atmosphere. For the assay, A549 and HeLa cells were seeded separately in 96-well plates at a density of 1×10^4 cells/well in 100 µL of their respective growth media. After 24 hours of incubation to allow adherence, the cells were treated with serial concentrations of:

- Free Etoposide
- Etoposide-loaded nanobubbles
- Blank nanobubbles at concentrations of 10, 25, 50, 75, and 100 µg/mL. Untreated cells served as the control.

Following 48 hours of incubation, 20 µL of MTT reagent (5 mg/mL) was added to each well, and the plates were further incubated for 4 hours. The medium was then discarded, and 100 µL of DMSO was added to solubilize the formazan crystals. Absorbance was recorded at 570 nm using a microplate reader. The percentage of viable cells was calculated using the formula {Präbst, 2017 #330;Pascua-Maestro, 2018 #331}:
Cell viability (%) was calculated using the formula:
Cell Viability (%) = {Absorbance of Treated Cells / Absorbance of Control Cells} ×100
Each experiment was performed in triplicate (n = 3), and the results were expressed as mean ± standard deviation (SD). The data were used to plot dose–response curves, and IC_{50} values were calculated using non-linear regression analysis.

2.6. Statistical Analysis

All experimental procedures were carried out in triplicate (n = 3) to ensure reliability and reproducibility of the results. Data were expressed as mean ± standard deviation (SD) for each group or measurement. For comparative analysis among multiple groups, one-way analysis of variance (ANOVA) was applied to determine statistical significance across different formulations and treatment conditions. Where significant differences were observed ($p < 0.05$), Tukey's post hoc test was performed to identify specific group differences. Statistical computations were carried out using GraphPad Prism (version 8.0) or an equivalent statistical software package. A p-value < 0.05 was considered indicative of statistical significance in all analyses.

3. RESULTS AND DISCUSSION

3.1. Characterization of Etoposide-Loaded Nanobubbles

As shown in Table 2, the average particle size of the nanobubble formulations ranged from 198.4 nm (F1) to 125.5 nm (F5). A consistent reduction in particle size was observed with increasing concentrations of phospholipid and cholesterol. This size reduction can be attributed to improved bilayer compaction and enhanced probe-sonication efficiency during formulation. All formulations exhibited low polydispersity index (PDI) values (<0.3), indicating a narrow and uniform particle size distribution, with F5 showing the most uniformity (PDI: 0.192). The zeta potential values ranged from –21.3 mV to –30.6 mV, indicating moderate to high colloidal stability due to electrostatic repulsion among particles. Formulation F5 showed the highest negative surface charge, suggesting improved long-term stability. Entrapment efficiency increased progressively from F1 (68.5%) to F5 (91.4%), which can be correlated with enhanced lipid content, providing greater bilayer capacity for drug incorporation. Similarly, drug loading was maximized in F5 (6.7%) due to improved encapsulation and tighter lipid packing.

Table 2. Characterization of Etoposide-Loaded Nanobubbles (Mean ± SD, n = 3)

Formulation Code	Particle Size (nm)	PDI	Zeta Potential (mV)	Entrapment Efficiency (%)	Drug Loading (%)

F1	198.4 ± 3.2	0.298 ± 0.01	–21.3 ± 1.1	68.5 ± 1.8	4.5 ± 0.2
F2	172.6 ± 2.9	0.267 ± 0.01	–24.5 ± 1.0	74.2 ± 2.0	5.1 ± 0.2
F3	151.2 ± 2.7	0.243 ± 0.01	–27.1 ± 0.9	81.7 ± 1.5	5.8 ± 0.3
F4	136.8 ± 2.3	0.214 ± 0.01	–28.8 ± 0.8	88.9 ± 1.2	6.2 ± 0.3
F5	125.5 ± 2.1	0.192 ± 0.01	–30.6 ± 0.7	91.4 ± 1.1	6.7 ± 0.2

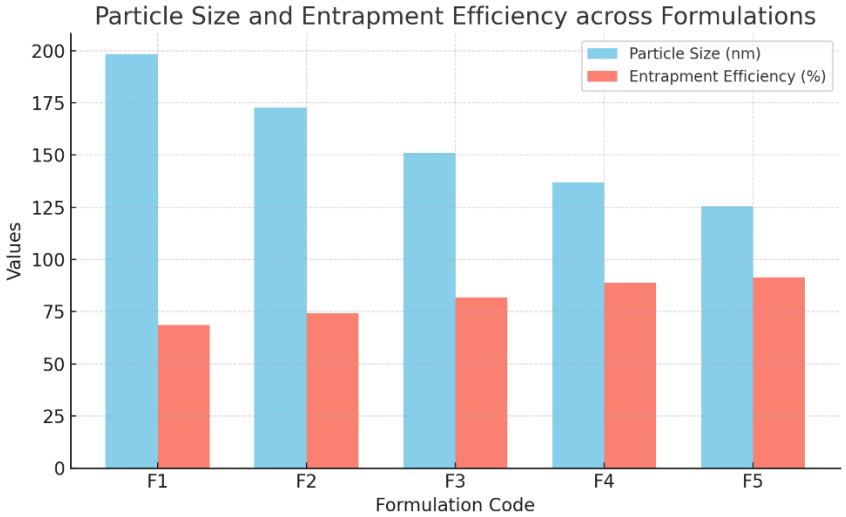

Figure 1: Bar graph of Particle Size and Entrapment Efficiency across Formulations F1–F5

3.1.1 Morphological study by TEM

The morphological evaluation of Etoposide-loaded nanobubbles was conducted using Transmission Electron Microscopy (TEM) to confirm their size, shape, and structural integrity. As shown in the TEM micrographs, the nanobubbles appeared as well-defined, discrete, and predominantly spherical vesicles with smooth surfaces and uniform distribution. The images revealed a consistent nanometric size range, corroborating the results obtained from dynamic light scattering (DLS). The core–shell architecture of the nanobubbles was clearly distinguishable, indicating successful encapsulation of the drug within the lipid bilayer surrounding the gas core. No aggregation or deformation was observed, suggesting that the formulation process yielded stable and monodisperse vesicles with intact morphology. The electron-dense outline of the lipid shell further supported the presence of a well-structured nanocarrier system. These observations confirm that the formulation method employed, thin-film hydration followed by probe sonication, was effective in producing morphologically uniform and structurally stable nanobubbles suitable for drug delivery applications. The nanoscale structure and spherical shape are particularly advantageous for enhanced cellular uptake, prolonged circulation, and tumor penetration via the enhanced permeability and retention (EPR) effect

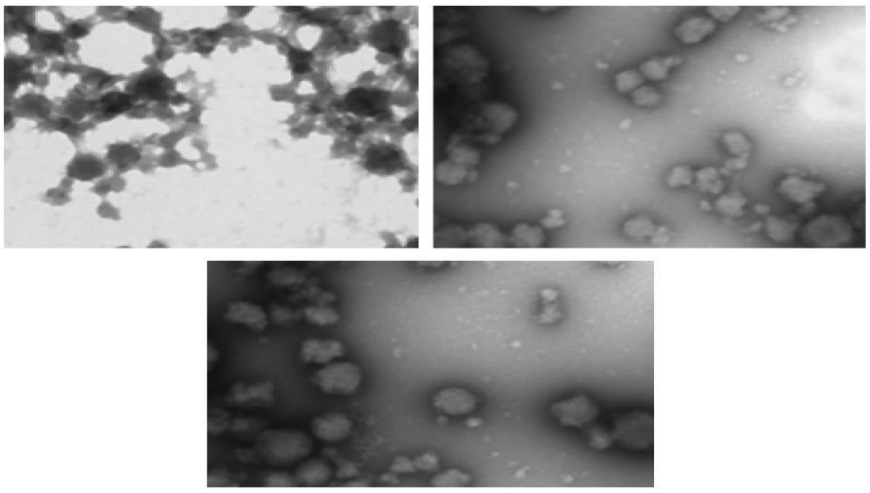

Figure 2. Representative TEM image of Etoposide-loaded nanobubbles showing spherical morphology and uniform distribution.

3.2. In Vitro Drug Release Profile

The cumulative drug release profiles presented in Table 3 reveal a sustained release behavior for all nanobubble formulations over a 48-hour period. F1 showed the fastest release (88.7%), while F5 demonstrated a controlled and prolonged release, reaching up to 99.4% at 48 hours. The extended release observed in F5 may be attributed to its smaller particle size and denser lipid bilayer, which restricts rapid diffusion of Etoposide. The release kinetics were indicative of a diffusion-controlled mechanism, and the formulations are suitable for sustained delivery applications in chemotherapy. The release profile of F5 suggests it as the optimal candidate for achieving prolonged systemic exposure and reducing dosing frequency.

Table 3. In Vitro Drug Release Profile of Etoposide-Loaded Nanobubbles (Mean ± SD, n = 3)

Time	F1 (%)	F2 (%)	F3 (%)	F4 (%)	F5 (%)
0.5 h	12.3 ± 0.5	10.6 ± 0.4	9.1 ± 0.4	7.8 ± 0.3	6.5 ± 0.3
1 h	19.8 ± 0.7	18.5 ± 0.6	16.2 ± 0.5	14.6 ± 0.4	13.4 ± 0.4
2 h	28.4 ± 0.6	26.7 ± 0.5	24.5 ± 0.5	22.9 ± 0.4	21.1 ± 0.4
4 h	42.7 ± 0.8	39.5 ± 0.7	36.8 ± 0.6	34.2 ± 0.6	32.4 ± 0.5
6 h	55.1 ± 0.9	52.4 ± 0.8	50.7 ± 0.7	49.3 ± 0.6	47.6 ± 0.5
8 h	63.9 ± 0.8	60.8 ± 0.7	58.6 ± 0.6	56.7 ± 0.6	55.9 ± 0.6
12 h	71.3 ± 0.9	70.2 ± 0.8	73.1 ± 0.7	75.4 ± 0.7	78.6 ± 0.6
24 h	82.1 ± 1.0	84.4 ± 0.9	87.2 ± 0.8	89.9 ± 0.8	92.3 ± 0.7
48 h	88.7 ± 1.1	90.6 ± 0.9	94.5 ± 0.8	97.8 ± 0.7	99.4 ± 0.6

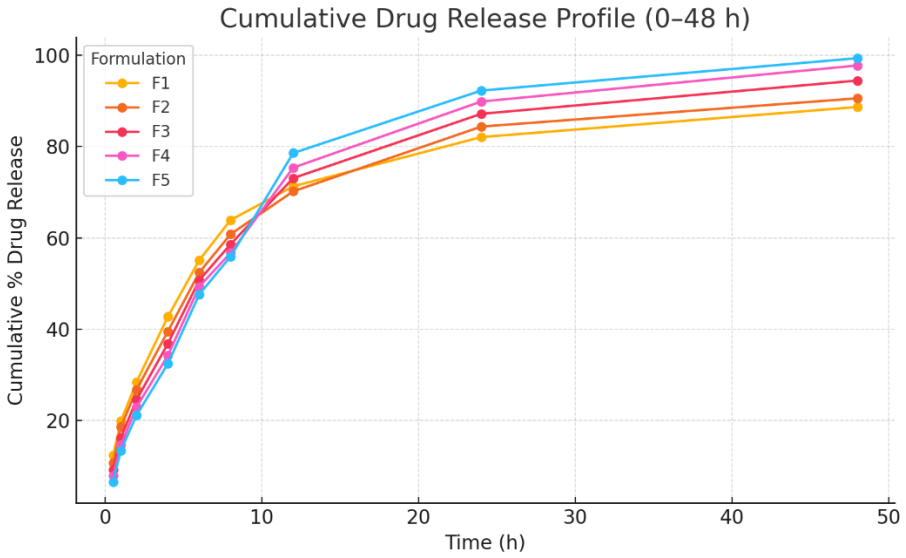

Figure 3: Line graph showing cumulative % drug release vs. time (0–48 h) for F1 to F5

3.2.1 Kinetic modelling of in vitro release data

The release data of Etoposide from nanobubble formulations F1 to F5 were fitted to various kinetic models, including Zero-order, First-order, Higuchi, and Korsmeyer–Peppas equations, to elucidate the release mechanism and rate-controlling steps. Among all models, the first-order model exhibited the best fit for all formulations, with correlation coefficients (r^2) ranging from 0.9932 (F1) to 0.9986 (F3). This clearly suggests that the release of Etoposide was concentration-dependent, a hallmark of first-order kinetics where the release rate decreases over time as the drug concentration inside the carrier diminishes. The Higuchi model also demonstrated moderate to good correlation (r^2 ~ 0.86 to 0.91), confirming that diffusion from a matrix system was one of the dominant mechanisms governing the release. The progressive improvement in Higuchi fit from F1 to F5 coincides with decreasing particle size and increasing lipid content, which can enhance the tortuosity of the diffusion path. The Korsmeyer–Peppas model, which is particularly useful for distinguishing between different diffusion and erosion mechanisms, provided an excellent fit for all formulations ($r^2 > 0.99$). The 'n' values for the model ranged from 0.5904 to 0.7280. For spherical particles, an 'n' value between 0.45 and 0.89 indicates anomalous (non-Fickian) diffusion, meaning the drug release was governed by a combination of diffusion and polymer relaxation (erosion) mechanisms. The optimized formulation, F5, exhibited the highest 'n' value (0.728) and a Korsmeyer–Peppas r^2 of 0.9954, suggesting that it followed slow, controlled release with strong matrix integrity. These findings reinforce the potential of nanobubbles as an effective sustained release system, particularly when tuned with the right lipid and stabilizer composition.

Table 4. Kinetic Modelling of In Vitro Drug Release Data

Formulation	Zero-Order (r^2)	First-Order (r^2)	Higuchi (r^2)	Korsmeyer-Peppas (r^2)	n (KP Model)
F1	0.6504	0.9932	0.8586	0.9991	0.5904
F2	0.6879	0.9967	0.8860	0.9971	0.6101
F3	0.7105	0.9986	0.9000	0.9974	0.6447
F4	0.7259	0.9971	0.9078	0.9952	0.6817
F5	0.7210	0.9940	0.9017	0.9954	0.7280

3.3. In Vitro Cytotoxicity (MTT Assay) IN MCF-7 cells

The cytotoxic potential of the formulations was evaluated using the MTT assay on MCF-7 breast cancer cells, with results summarized in Table 5. The Etoposide-loaded nanobubbles exhibited significantly enhanced cytotoxicity compared to free Etoposide at all tested concentrations. At the highest concentration (100 µg/mL), the nanobubbles reduced cell viability to 18.9%, compared to 31.4% for free Etoposide, demonstrating superior cellular uptake and retention of the nanocarrier system. Blank nanobubbles showed negligible cytotoxicity (cell viability >94% across all concentrations), confirming the biocompatibility of the lipid components. The improved anticancer activity of the Etoposide-loaded nanobubbles can be

attributed to sustained drug release, better cellular internalization, and increased residence time at the site of action.

Table 5. In Vitro Cytotoxicity on MCF-7 Cells After 48 h (MTT Assay, Mean ± SD, n = 3)

Concentration	Free Etoposide (%)	Etoposide-Loaded Nanobubbles (%)	Blank Nanobubbles (%)
10 µg/mL	84.6 ± 2.3	78.9 ± 2.1	97.8 ± 1.2
25 µg/mL	71.3 ± 2.1	63.4 ± 1.9	96.5 ± 1.1
50 µg/mL	59.2 ± 1.8	48.1 ± 1.7	95.3 ± 1.0
75 µg/mL	45.7 ± 1.6	32.6 ± 1.4	94.8 ± 0.9
100 µg/mL	31.4 ± 1.3	18.9 ± 1.2	94.1 ± 0.8

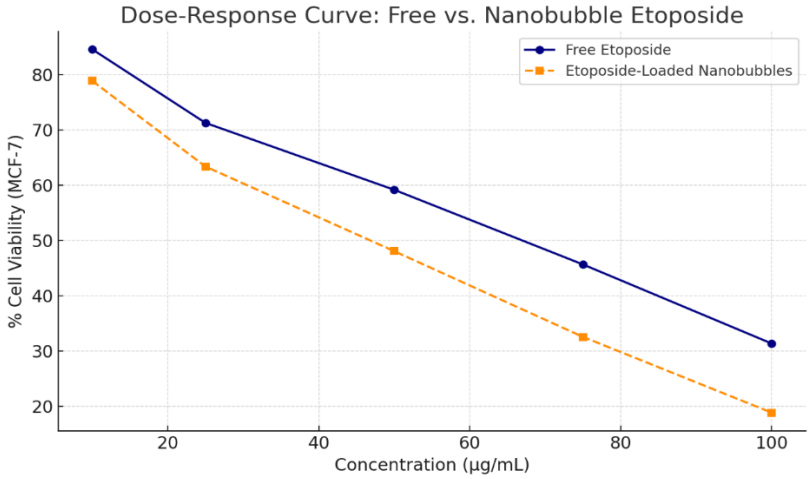

Figure 4: Dose-response curve showing % cell viability vs. Etoposide concentration (Free vs. Nanobubble)

3.4. In Vitro Cytotoxicity Against A549 Cells

The cytotoxic effects of Etoposide-loaded nanobubbles were further validated on A549 lung carcinoma cells using the MTT assay (Table 6). A dose-dependent decrease in cell viability was observed for both free Etoposide and nanobubble formulations, with the latter showing significantly enhanced cytotoxicity at all concentrations. At 100 µg/mL, nanobubbles reduced cell viability to 19.8 ± 1.2%, compared to 30.7 ± 1.3% for free Etoposide. This enhancement can be attributed to improved cellular uptake, sustained release, and enhanced intracellular retention of the drug delivered via nanobubbles. Blank nanobubbles exhibited negligible cytotoxicity across the tested range (cell viability >94%), confirming their excellent biocompatibility with A549 cells. The IC_{50} of Etoposide-loaded nanobubbles was clearly lower than that of the free drug, suggesting superior anti-proliferative potential of the formulation. These results align with the hypothesis that nanobubble encapsulation can significantly improve the therapeutic index of Etoposide in lung cancer treatment models.

Table 6. In Vitro Cytotoxicity on A549 Cells After 48 h (MTT Assay, Mean ± SD, n = 3)

Concentration	Free Etoposide (%)	Etoposide-Loaded Nanobubbles (%)	Blank Nanobubbles (%)
10 µg/mL	86.1 ± 2.4	79.4 ± 2.2	98.2 ± 1.1
25 µg/mL	73.8 ± 2.1	65.2 ± 2.0	96.9 ± 1.0
50 µg/mL	60.2 ± 1.8	50.3 ± 1.7	95.6 ± 0.9
75 µg/mL	44.5 ± 1.6	34.1 ± 1.5	95.0 ± 0.9
100 µg/mL	30.7 ± 1.3	19.8 ± 1.2	94.4 ± 0.8

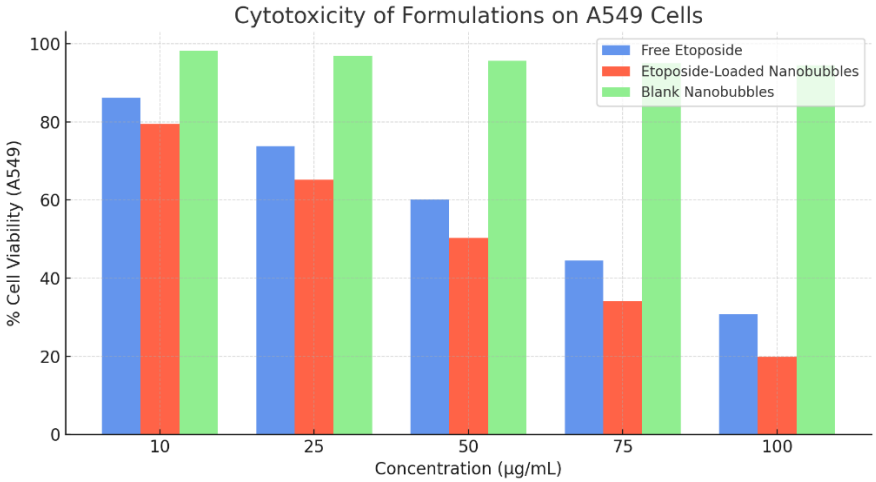

Figure 5: Bar graph showing cell viability (%) of A549 cells vs. concentration for Free Drug, Nanobubble, and Blank.

3.5. In Vitro Cytotoxicity Against HeLa Cells

The cytotoxic potential of the nanobubble formulation was also evaluated in HeLa cervical cancer cells (Table 7). Consistent with observations in MCF-7 and A549 cells, the Etoposide-loaded nanobubbles showed superior anticancer activity compared to the free drug. At 100 µg/mL, the nanobubbles reduced HeLa cell viability to 17.2 ± 1.1%, while free Etoposide resulted in 28.6 ± 1.2% viability. This enhanced response suggests that nanobubble-based delivery enables better intracellular trafficking and drug bioavailability. Blank nanobubbles again showed minimal cytotoxicity, with cell viability above 94% at all doses, reinforcing their safety profile. The improved cytotoxic response of the nanobubble system in HeLa cells supports the versatility of this delivery platform across multiple cancer types, including those that may exhibit drug resistance.

Table 7. In Vitro Cytotoxicity on HeLa Cells After 48 h (MTT Assay, Mean ± SD, n = 3)

Concentration	Free Etoposide (%)	Etoposide-Loaded Nanobubbles (%)	Blank Nanobubbles (%)
10 µg/mL	82.7 ± 2.5	76.1 ± 2.3	97.5 ± 1.2
25 µg/mL	70.5 ± 2.2	61.8 ± 2.1	96.3 ± 1.0
50 µg/mL	58.3 ± 1.9	46.4 ± 1.8	95.0 ± 0.9
75 µg/mL	43.9 ± 1.6	30.7 ± 1.4	94.5 ± 0.9
100 µg/mL	28.6 ± 1.2	17.2 ± 1.1	94.0 ± 0.8

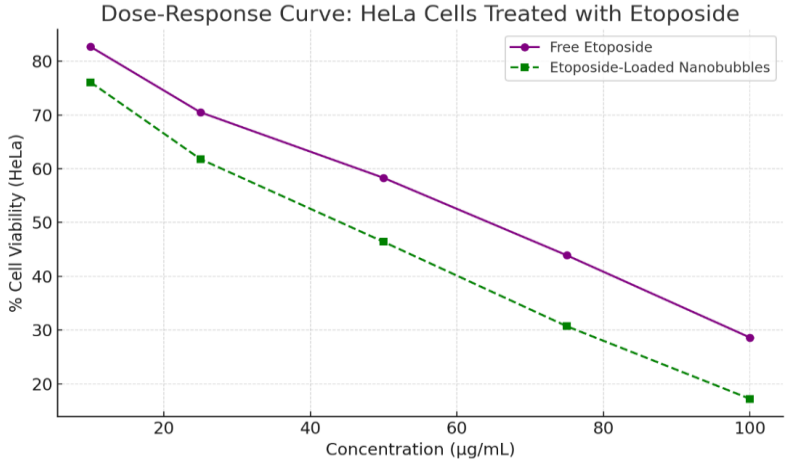

Figure 6: Line graph or dose–response curve for HeLa cells treated with Free Etoposide vs. Nanobubbles.

4. CONCLUSION

The present study successfully demonstrated the formulation, optimization, and evaluation of Etoposide-loaded nanobubbles as a novel drug delivery system for cancer therapy. The nanobubbles were prepared using a modified thin-

film hydration and sonication method, resulting in stable, nanosized vesicles with suitable physicochemical properties. Among the five formulations (F1–F5), formulation F5 emerged as the most optimized, exhibiting a uniform particle size of 125.5 ± 2.1 nm, low polydispersity index, high zeta potential (–30.6 ± 0.7 mV), and superior entrapment efficiency (91.4 ± 1.1%). These attributes collectively suggest that F5 possessed desirable characteristics for efficient drug delivery and prolonged systemic circulation. In vitro release studies further confirmed the sustained release behaviour of the optimized formulation, achieving 99.4 ± 0.6% cumulative drug release over 48 hours. Kinetic modelling indicated that the drug release followed first-order kinetics, with strong fit to the Korsmeyer–Peppas model. The calculated 'n' values suggested a non-Fickian, anomalous release mechanism driven by both diffusion and erosion processes.

The cytotoxic potential of the nanobubbles was evaluated in MCF-7, A549, and HeLa cancer cell lines using the MTT assay. In all models, Etoposide-loaded nanobubbles demonstrated significantly enhanced cytotoxicity compared to the free drug, particularly at higher concentrations, while blank nanobubbles showed minimal toxicity, highlighting their biocompatibility. The enhanced activity of the nanobubbles can be attributed to better intracellular uptake, controlled release, and increased local drug concentration within tumor cells. In conclusion, Etoposide-loaded nanobubbles offer a promising strategy for improving the therapeutic efficacy and safety of anticancer agents. Their ability to sustain drug release, enhance cytotoxicity, and remain biocompatible underscores their potential for further preclinical and clinical development as a targeted delivery system for cancer treatment. Future work may include in vivo pharmacokinetic studies and tumor-targeting enhancements using ligand conjugation

REFERENCES

. Ahsan, A., Thomas, N., Barnes, T. J., Subramaniam, S., Loh, T. C., Joyce, P., & Prestidge, C. A. (2024). Lipid Nanocarriers-Enabled Delivery of Antibiotics and Antimicrobial Adjuvants to Overcome Bacterial Biofilms. Pharmaceutics, 16(3). https://doi.org/10.3390/pharmaceutics16030396

[2] Bailly, C. (2023). Etoposide: A rider on the cytokine storm. Cytokine, 168, 156234. https://doi.org/10.1016/j.cyto.2023.156234

[3] Charbgoo, F., Ahmad, M. B., & Darroudi, M. (2017). Cerium oxide nanoparticles: green synthesis and biological applications. Int J Nanomedicine, 12, 1401-1413. https://doi.org/10.2147/ijn.S124855

[4] Cordani, M., Dando, I., Ambrosini, G., & González-Menéndez, P. (2024). Signaling, cancer cell plasticity, and intratumor heterogeneity. Cell Commun Signal, 22(1), 255. https://doi.org/10.1186/s12964-024-01643-5

[5] Cui, H., & Smith, A. L. (2022). Impact of engineered nanoparticles on the fate of antibiotic resistance genes in wastewater and receiving environments: A comprehensive review. Environ Res, 204(Pt D), 112373. https://doi.org/10.1016/j.envres.2021.112373

[6] Dolgin, E. (2021). Cancer's new normal. Nat Cancer, 2(12), 1248-1250. https://doi.org/10.1038/s43018-021-00304-7

[7] Fleming, R. A., Miller, A. A., & Stewart, C. F. (1989). Etoposide: an update. Clin Pharm, 8(4), 274-293.

[8] Hainsworth, J. D., & Greco, F. A. (1995). Etoposide: twenty years later. Ann Oncol, 6(4), 325-341. https://doi.org/10.1093/oxfordjournals.annonc.a059180

[9] Hande, K. R. (1992). Etoposide pharmacology. Semin Oncol, 19(6 Suppl 13), 3-9.

[10] Hashida, M. (2022). Advocation and advancements of EPR effect theory in drug delivery science: A commentary. J Control Release, 346, 355-357. https://doi.org/10.1016/j.jconrel.2022.04.031

[11] Hausman, D. M. (2019). What Is Cancer? Perspect Biol Med, 62(4), 778-784. https://doi.org/10.1353/pbm.2019.0046

[12] Issell, B. F., & Crooke, S. T. (1979). Etoposide (VP-16-213). Cancer Treat Rev, 6(2), 107-124. https://doi.org/10.1016/s0305-7372(79)80045-6

[13] Kroemer, G., & Pouyssegur, J. (2008). Tumor cell metabolism: cancer's Achilles' heel. Cancer Cell, 13(6), 472-482. https://doi.org/10.1016/j.ccr.2008.05.005

[14] Markman, J. L., Rekechenetskiy, A., Holler, E., & Ljubimova, J. Y. (2013). Nanomedicine therapeutic approaches to overcome cancer drug resistance. Adv Drug Deliv Rev, 65(13-14), 1866-1879. https://doi.org/10.1016/j.addr.2013.09.019

[15] Rajakumar, G., & Abdul Rahuman, A. (2011). Larvicidal activity of synthesized silver nanoparticles using Eclipta prostrata leaf extract against filariasis and malaria vectors. Acta Trop, 118(3), 196-203. https://doi.org/10.1016/j.actatropica.2011.03.003

[16] Roy, P. S., & Saikia, B. J. (2016). Cancer and cure: A critical analysis. Indian J Cancer, 53(3), 441-442. https://doi.org/10.4103/0019-509x.200658

[17] Shi, Y., van der Meel, R., Chen, X., & Lammers, T. (2020). The EPR effect and beyond: Strategies to improve tumor targeting and cancer nanomedicine treatment efficacy. Theranostics, 10(17), 7921-7924.

https://doi.org/10.7150/thno.49577

..